DOI 10.5012/bkcs.2010.31.02.423

Preparation and Electrochemical Performance of CNT Electrode with Deposited Titanium Dioxide for Electrochemical Capacitor

Hong-Il Kim, Han-Joo Kim,† Masayuki Morita,‡ and Soo-Gil Park*

Department of Industrial Engineering Chemistry, Chungbuk National University, Cheong-ju 361-763, Korea
**E-mail: sgpark@cbnu.ac.kr*
†Pureechem Co., Ltd., Cheong-ju 361-763, Korea
‡Department of Applied Chemistry, Graduate School of Science and Engineering, Yamaguchi-University, 2-16-1 Tokiwadai, Ube 755-8611, Japan
Received April 15, 2009, Accepted January 9, 2010

To reduce polarization of electrochemical capacitor based on carbon nanotube, titanium oxide nanoparticles were deposited by ultrasound. The pore distribution of TiO_2/CNT nanoparticle exhibited surface area of 341 m^2g^{-1} when TiO_2 content was 4 wt %, which was better than that of pristine CNT with surface area of 188 m^2g^{-1}. The analyses indicated that titanium oxide (particle diameter < 20 nm) was deposited on the CNT surface. The electrochemical performance was evaluated by using cyclic voltammetry (CV), impedance measurement, and constant-current charge/discharge cycling techniques. The TiO_2/CNT composite electrode showed relatively better electrochemical behaviors than CNT electrode by increasing the specific capacitance from 22 Fg^{-1} to 37 Fg^{-1} in 1 M H_2SO_4 solution. A symmetric cell assembled with the composite electrodes showed the specific capacitance value of 11 Fg^{-1} at a current loading of 0.5 $mAcm^{-2}$ during initial cycling.

Key Words: Electrochemical capacitor, Titanium dioxide, CNT, Polarization

Introduction

Electrochemical capacitor is an electrochemical energy storage device utilizing the electric charges accumulated at the interface between the electrode and the electrolyte to form the electric double layer.[1-5] It has been increasingly getting attention not only for the established applications as backup power to electronic equipments and mobile devices,[6,7] but also for high power applications in pulsed lasers and electric vehicles.[8,9]

Advancement in energy-storage technologies can benefit from the shift from conventional to nanostructured electrodes. For electrochemical capacitors, focus has been on nanostructured carbons, nanotubes, and nanotemplates.[10,11] Among these materials, carbon nanotubes (CNTs) have been considered ideal for electrochemical capacitors, owing to the advantages such as accessible surface area, excellent electronic conductivity, and good stability.[12-17]

On the other hand, CNT grows the polarization when CNT electrode reacts with electrolyte through the electrode/electrolyte interface. Generally, polarization is the change of potential of an electrode from its equilibrium potential upon the application of a current. The phenomenon of transportation of electrical charge from one part of the electrochemical cell to another, occurring mainly as electromigration of ions, but it can also occur by diffusion of ions.[5,17] The specific capacitance of the electrochemical capacitor based on CNTs has been reported to present lower capacitance of about 20 ~ 30 Fg^{-1}. The lower capacitance is partially attributed to poor wettability of electrode material, which leads to a lower usable specific surface area for charge storage.[18] As another reason, polarization may reduce charge accumulation of the ions on the double-layer. For these reasons, reducing the polarization of activated carbon by introducing TiO_2 nanoparticles has been considered to be an effective approach to improve the capacitance of the double-layer capacitors.[5] In this study, we considered that wettability and polarization of the nanocomposite electrode depend on the content of TiO_2 deposited on CNT.

Experimental

The TiO_2/CNT nanocomposite material was prepared by sol-gel process with ultrasound in 2-propanol. The starting material, titanium isopropoxide (Aldrich Co., Ltd.) was commercially available with purity of 99%. The average outer diameter of CNT (MWNT type, Iljinnanotech. Co., Ltd.) was 15 ~ 20 nm and the length was 10 ~ 20 μm. The CNT was chemically oxidized in 1M H_2SO_4 for 48 h at 80 °C and dried at 120 °C overnight. Titanium isopropoxide (0.2, 0.4, 0.6 and 0.8 M) and 1 g CNTs were mixed in 2-propanol (200 mL) with ultrasound, respectively. Then they were mixed with stirring under ultrasound for 30 min. The mixture was separated from the solvent by drying at 90 °C into vacuum oven overnight. The resultant was calcinated at 450 °C for 2 h in air at a heating rate of 5 °C/min to form TiO_2/CNT nanocomposite. The samples were characterized by X-ray diffraction (XRD, SCINTAG DMS2000) and transmission electron microscope (TEM, model Joel-1020 Carl Zeiss TEM109) was used to monitor the particle size at each synthesis step. X-ray Photoelectron Spectroscopy (XPS, ESCALAB 210) was used to obtain the structure of nanocomposite.

The working electrode was prepared from a mixture paste of TiO_2/CNT nanocomposite powder, ketijen black(KB) as an electronic conductor additive, and polyvinylidene fluoride (PVdF) binder mixed with the weight ratio of 85:10:5 in *N*-Methyl-2-Pyrrolidone (NMP). The electrode was dried under vacuum

at 120 °C for 24 h before electrochemical evaluation. Electrochemical measurements were conducted using conventional three-electrode configuration and symmetrical full cell. The TiO_2/CNT composite on carbon paper electrode was used as the working electrode. A Pt wire and KCl-saturated Ag/AgCl were used as the counter and reference electrodes, respectively. The 1M H_2SO_4 aqueous solution was used as the electrolyte. Cyclic voltammetry (CV) was measured on range of 0 ~ 800 mV. Scan rate was 50mVs^{-1} and it was shown after 3 th cycle. And cycling performance of the two electrodes in cell was measured at 0.5 mAcm^{-2} between 0 and 1000 mV. All the measurements were taken at room temperature and under nitrogen atmosphere.

Results and Discussion

In order to show actual size and formation of deposited TiO_2 particle, Fig. 1 (b) ~ (e) present TEM images of TiO_2/CNT composite materials with different TiO_2 weight ratio. Some of the shapes of these samples were classified as a part of a straight form with a thick outer diameter and another rest as a curved style with a narrow outer diameter. The TiO_2/CNT composite materials were different from the result in Fig. 1. From above results, our attempt to prepare the TiO_2/CNT composite materials was successful. And the more the TiO_2 was inserted, the more the deposited TiO_2 grains clumped together. The particles are spherical with the size of about 10 ~ 20 nm in diameter.

Fig. 2 shows the X-ray diffraction (XRD) patterns of the CNT and the CNT on which TiO_2 was deposited with contents of 4, 6, 17, and 32 wt %. After the stoichiometric precursor of TiO_2/CNT composite has been calcinated at 450 °C for 2 h in air, the anatase phase of TiO_2 has been appeared. The peaks located at 25.66° and 42.50° could be identified to the reflection from the (002) and (100) planes of CNT and the additional peaks observed at 25.07°, 37.66°, 47.74°, 53.8°, 54.29° and 62.44° are corresponding to (101), (004), (200), (105), (211) and (204) planes of anatase TiO_2 (JCPDS no. 21-1272).[19] All of broaden and weaken peaks in Fig. 2 imply that TiO_2/CNT composite materials consisted of TiO_2 and CNT nanoparticles belong to low-dimensional states. The CNT (002) reflection overlaps the anatase TiO_2 (101) reflection. As is seen in Fig. 2, the TiO_2/CNT composite shows CNT peak, and also anatase peaks of the composites grow as the TiO_2 content increases. And no peak of other phases was observed, which indicates that the composite materials are well crystallized.

The X-ray photoelectron spectroscopy (XPS) which was performed to investigate the chemical bonding state of Ti in the TiO_2/CNT composite material prepared at 450 °C for 2 h is shown in Fig. 3. The Ti 2p signal of the TiO_2/CNT composites shows a Ti $2p_{1/2}$ peak centered at 464.8 eV and a Ti $2p_{3/2}$ peak at 459 eV. The observed binding energies (B.E.) of Ti $2p_{1/2}$ and Ti $2p_{3/2}$ peaks for TiO_2/CNT composites are near to those observed for TiO_2 (458.5 and 464.2 eV, respectively). The atomic % of TiO_2 nanoparticle (C_x) was calculated peak area from the equation (1):

$$C_x \text{ atomic } \% = [(I_i / F_i) / \Sigma(I / F)] \times 100 \quad (1)$$

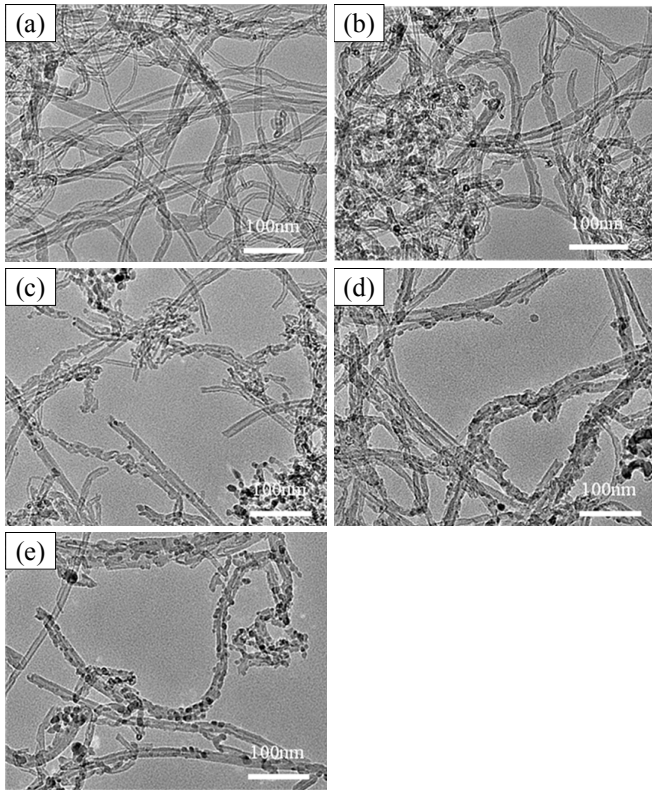

Figure 1. TEM images of (a) the pristine CNT and TiO_2/CNT nanocomposites with deposited TiO_2 contents of (b) 4 wt %, (c) 6 wt %, (d) 17 wt % and (e) 32 wt %.

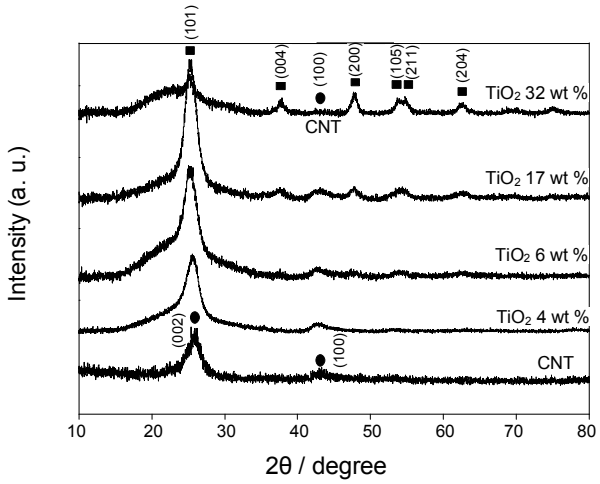

Figure 2. X-ray diffraction patterns (Cu Kα) of the pristine CNT and TiO_2/CNT nanocomposites with various TiO_2 contents.

where I is the number of photoelectron per second in a specific spectra peak, F is the atomic sensitivity factor, i is the TiO_2 element. According to the XPS results, TiO_2/CNT composites contained TiO_2 particle of correctly 4 wt %, 6 wt %, 17 wt % and 32 wt % on CNT, respectively.

Fig. 4 shows the nitrogen adsorption isotherms of the (a) CNT and the CNT on which TiO_2 was deposited with contents of (b) 4, (c) 6, (d) 17, and (e) 32 wt %. An increase in the TiO_2 con-

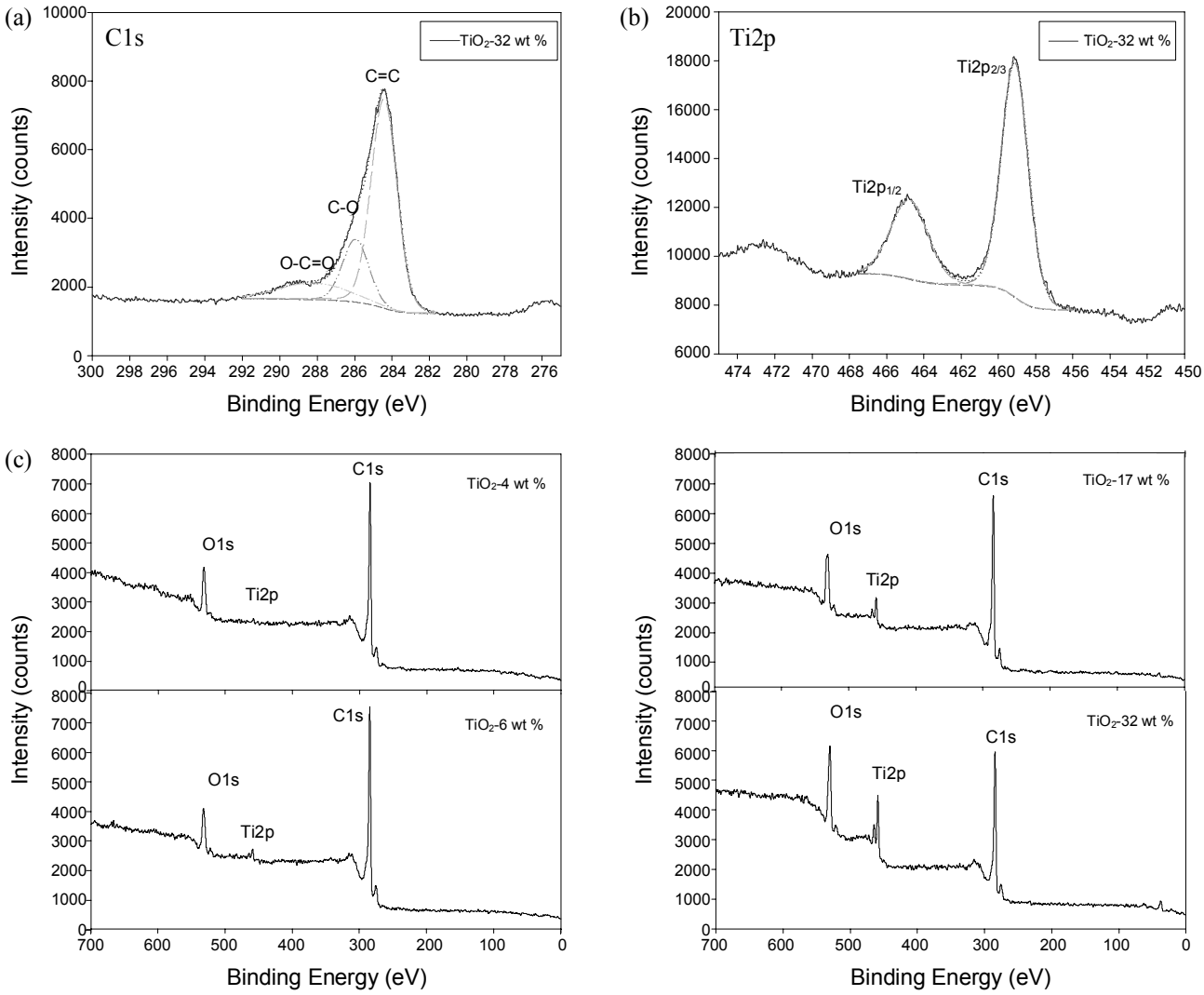

Figure 3. The X-ray photoelectron spectroscopic scans of the pristine CNT and TiO_2/CNT nanocomposites with various TiO_2 contents. (a) C1s (32 wt %), (b) Ti2p (32 wt %), and (c) wide scans of TiO_2/CNT nanocomposites.

tents a great enhancement in the nitrogen adsorption capacity. Fig. 5 shows the BET surface area of the pristine CNT and TiO_2/CNT nanocomposites with various deposited TiO_2 contents. After deposition of TiO_2, surface area raises the porosity of the TiO_2/CNT composite to improve BET specific surface area. When comparing those TiO_2/CNT composites, 4 wt % TiO_2/CNT composites and 6 wt % TiO_2/CNT composites have higher specific surface area. The pore distribution of TiO_2/CNT nanocomposites is exhibited in Table 1. As seen in this Table, the 4 wt % and 6 wt % TiO_2/CNT composites showed most excellent values of specific surface area (341 m^2g^{-1}) and micro pore area (17 m^2g^{-1}) compared with the pristine CNT, respectively. But higher contents of deposited TiO_2 decreased both specific surface area and micro pore area.

The effect of TiO_2 on the capacitance property of the TiO_2/CNT composite material was measured by cyclic voltammetry. Fig. 6 shows the cyclic voltammograms in 1 M H_2SO_4 electrolyte in the range of 0 ~ 800 mV at 50 mVs^{-1}. In order to determine a good composition ratio of the TiO_2/CNT electrode, the capacitances with different ratios of TiO_2 contents were measured in 1M H_2SO_4. The specific capacitance C_s can be calculated from the cyclic voltammetry according to the equation (2):

$$C_s = [(i_c + i_a) / 2 / \upsilon] / w \quad (2)$$

where i_c and i_a are currents at 0.0 V during the cathodic and anodic sweeps, respectively, υ is the sweep rate, and w is the total weight of the active material in one electrode. The anomalous increase in the current was caused by an enhancement of the electronic and/or ionic transfer between TiO_2/CNT nanocomposite electrode and electrolyte. When TiO_2 content was small, its double layer capacitance was only slightly higher than that of pristine CNT. But with increasing the TiO_2 content ratio, the capacitance was decreased on account of improvement in diffusion resistance from impedance analysis of Fig. 7. From the result, we suggest the optimized content of TiO_2 to be 4 wt % in H_2SO_4 electrolyte. The specific capacitance of the pristine CNT and TiO_2/CNT composite electrodes are listed in Table 1. The 4 wt % TiO_2/CNT composite electrode delivered a specific capacitance of 37 Fg^{-1} which is higher than CNT electrode by 15 Fg^{-1}.

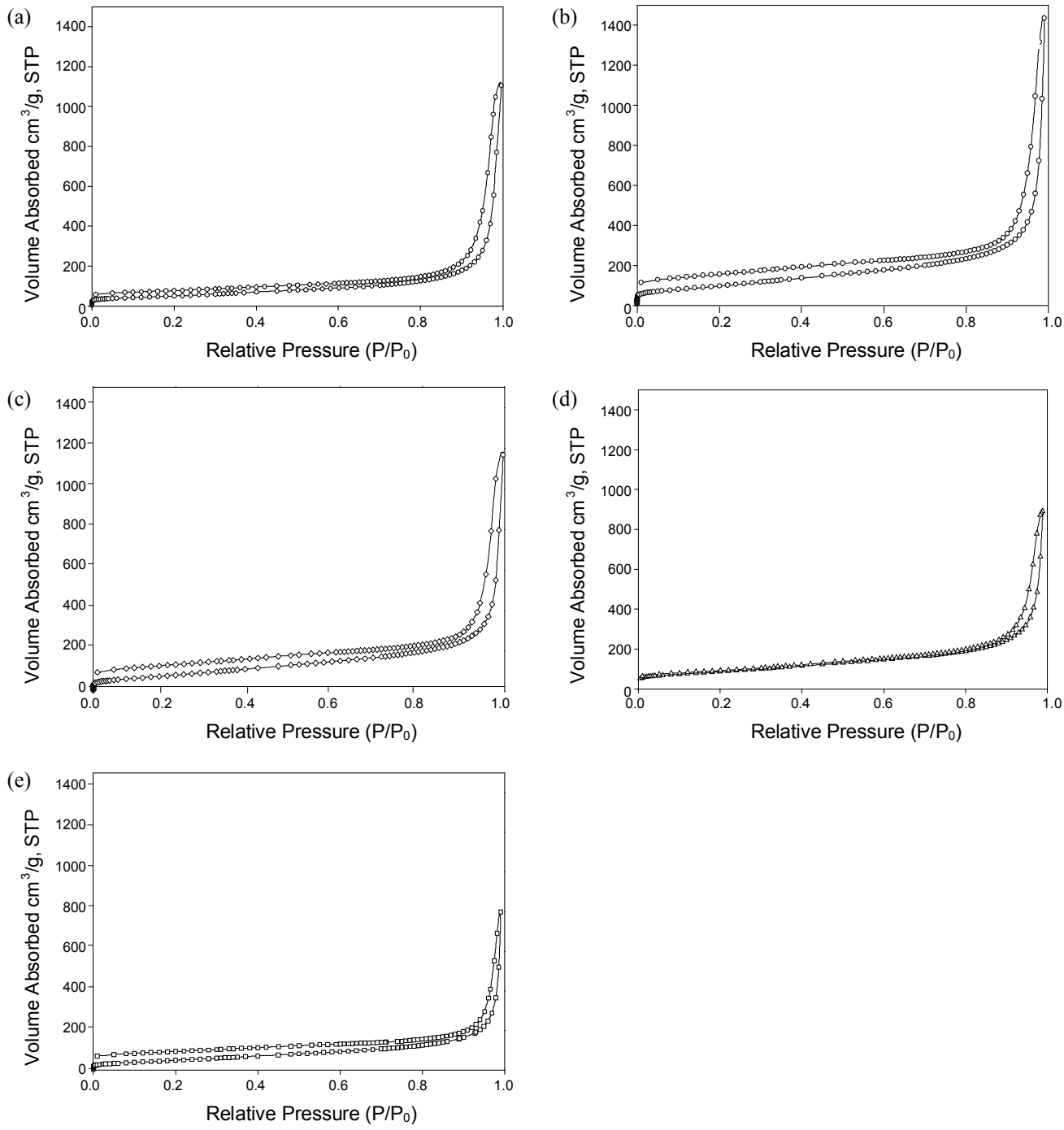

Figure 4. Nitrogen adsorption/desorption isotherms of the (a) the pristine CNT and TiO_2/CNT nanocomposites with deposited TiO_2 contents of (b) 4 wt %, (c) 6 wt %, (d) 17 wt % and (e) 32 wt %.

It has been reported[20] that the capacitance of an electrochemical capacitor is proportional to ion concentration and inversely proportional to the thickness of the double-layer, and the ion concentration is affected by the voltage between CNT electrodes and electrolyte. Based on above results, the increase of the capacitance in Table 1 could be attributed to the reduced polarization of CNT electrodes, which is believed to relate to the concentration of electric charges on TiO_2 surface with increasing wettability. And electric field adsorption of electrolyte on the CNT composite electrode was significantly enhanced by TiO_2 introduction due to the increase in the charge density of ions under electric field.[21]

A more detailed estimation of the electrochemical properties of the pristine CNT and TiO_2/CNT composite electrodes can be carried out by analysis of the impedance spectra. Fig. 7 shows Nyquist plots of the pristine CNT and TiO_2/CNT composite electrodes in 1M H_2SO_4. The plot is composed of a semicircle at high frequency and a nearly vertical line at low frequency. The

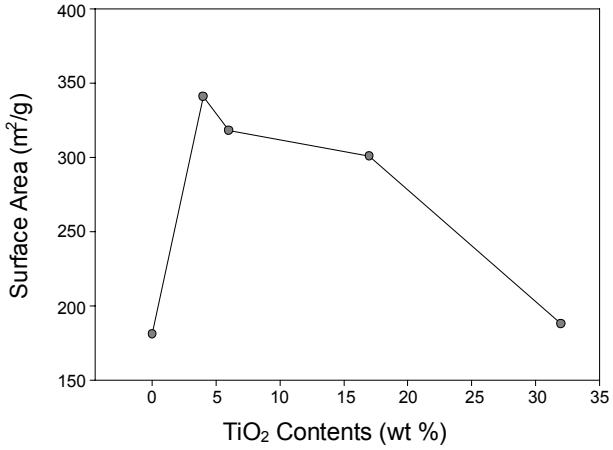

Figure 5. BET Surface area of the pristine CNT and TiO_2/CNT nanocomposites with various deposited TiO_2 contents.

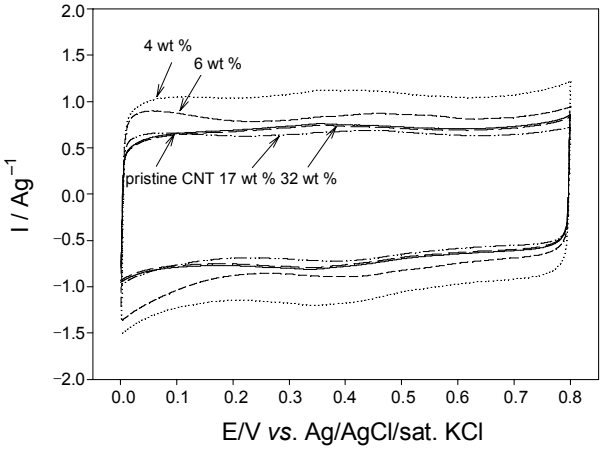

Figure 6. Cyclic voltammograms of the pristine CNT and TiO_2/CNT composite electrodes at scan rate of 50 mVs^{-1} in 1M H_2SO_4 electrolyte.

Table 1. BET surface area, specific capacitance and discharge capacitance of the CNT and TiO_2/CNT nanocomposites

Content (TiO_2 wt %)	BET (m^2g^{-1})	Micro pore area (m^2g^{-1})	Specific capacitance (Fg^{-1})	Discharge capacitance (Fg^{-1})
0	181	10	22	8
4	341	13	37	11
6	318	17	30	9
17	301	13	22	8
32	188	2	23	5

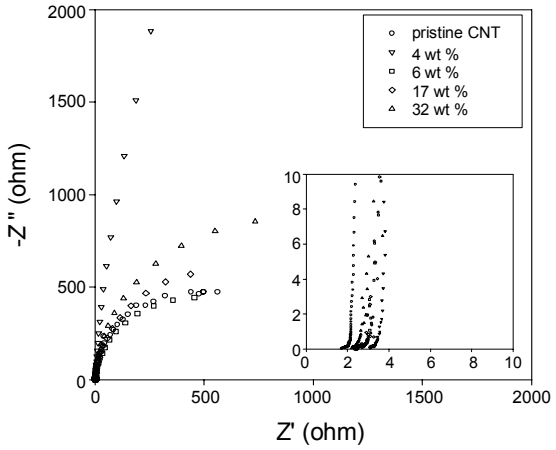

Figure 7. Nyquist plots of the pristine CNT and TiO_2/CNT nanocomposites with various deposited TiO_2 contents.

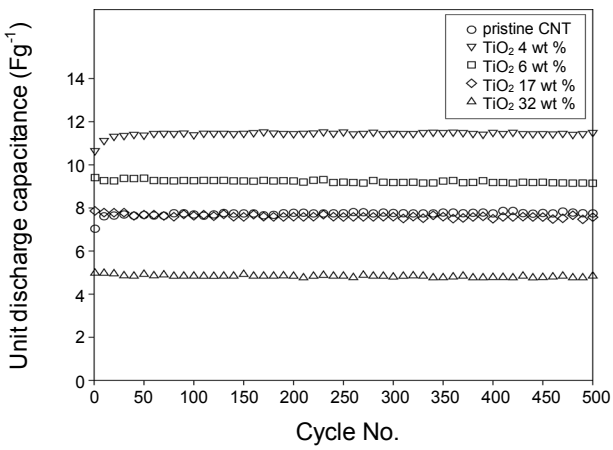

Figure 8. Cycle life performance of the pristine CNT and TiO_2/CNT electrodes at 0.5 $mAcm^{-2}$ in 1M H_2SO_4 electrolyte.

high frequency intercepts the real-axis bulk resistance of composite electrodes. The semicircle consists of electrode resistance of the pristine CNT and TiO_2/CNT composite electrodes. The bulk resistance of the capacitor built from CNT electrode was 1.7 ~ 1.8 Ω at 5.6 kHz. The resistances of the CNT electrodes with TiO_2 ratio of 4 wt %, 6 wt %, 17 wt % 32 wt % showed 3.8, 2.3, 2.4 and 2.4 Ω at 7.9, 12.5, 7.9 and 5 kHz, respectively. The resistances of the electrode/electrolyte interface on TiO_2/CNT composite electrodes were slightly higher than CNT electrode. The considerable effect of the Warburg impedance on the 4 wt % TiO_2/CNT composite electrode shows a good capacitor-like behavior of near vertical slope to 10 mHz. The Warburg impedance represents that the more the sloping line nears to the imaginary-axis, the more bulk resistance decreases. A Warburg diffusion element is incorporated in the circuit to emphasize the distributed resistance for ion diffusion in the micropores.[22] The results indicate that the composite material reduced the polarization and improved the hydrophilicity of the CNT surface, resulting in the decrease of internal resistance between electrode and electrolyte and increase of the efficiency of charge and mass-transfer on the electrode/electrolyte interface.[5]

This result of Nyquist plot agreed well with that from the cycle life performance. Fig. 8 shows the variation in unite discharge capacity as a function of cycle number (voltage range

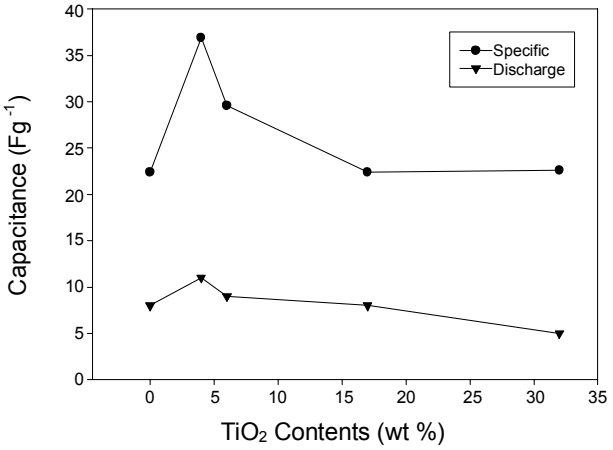

Figure 9. The effect of the contents of TiO_2 nanoparticle on the capacitance.

between 0 and 1 V, at 0.5 mAcm^{-2}). The discharge capacitance (C_d) was calculated from the equation (3):

$$C_d\ (\mathrm{Fg}^{-1}) = i\Delta t / m\Delta V \quad (3)$$

where i is the current density, Δt is the discharge time, m is the mass of the composite material, and ΔV is the potential range of the charge–discharge cycle. Regardless of the TiO_2 contents, symmetric cells showed the similar variation trend in unit discharge capacity with cycle : all capacitances showed a small loss in the first 10 cycles, and then remained almost constant as cycling continued. The average values of unit discharge capacity for the TiO_2/CNT composite electrodes and CNT electrode are listed in Table 1. The electrodes with 4 wt % and 6 wt % deposited TiO_2 not only delivered a unite discharge capacity of 11 Fg^{-1} and 9 Fg^{-1}, respectively, but also maintained an excellent cycling stability.

The dependence of specific capacitance on TiO_2 contents is shown in Fig. 9. The CNT composite electrode with 4 wt % of deposited TiO_2 shows higher capacitance and surface area than pristine CNT. From the result, it is indicated that increasing surface area and reducing polarization increase specific capacitance of CNT with TiO_2 nanoparticle. Table 1 summarizes the values of all the surface area and capacitance for the TiO_2/CNT composite electrodes along with the pristine CNT.

Conclusion

In the present work, CNT-based TiO_2 nanocomposites were successfully prepared by a simple method using ultrasound, and TiO_2 nanoparticles (< 20 nm) were partly deposited onto CNT. Nanocomposites electrodes with 4 ~ 6 wt % of deposited TiO_2 presented a better BET surface area compared with the pristine CNT. From Potentiostat/Galvanostat measurements in 1M H_2SO_4 aqueous solution, the specific capacitance and electrochemical performance improved through titanium oxide composition introduction. The specific capacitance of the composite electrode increased from 22 Fg^{-1} to 37 Fg^{-1} in comparison with the pristine CNT from cyclic voltammogram. And cycle life performance of the symmetric cell showed increase in capacitance from 8 Fg^{-1} to 11 Fg^{-1} and maintained an excellent cycling stability. We suggest the optimized content of TiO_2 to be 4 wt % and the increase in specific capacitance can be attributed to the decrease in electric polarization, caused by the deposition of TiO_2 nanoparticles on the CNT. This conclusion is supported by the Warburg impedance behavior showed near vertical slope to 10 mHz.

Acknowledgments. This work was financially supported by KOSEF through the Research Center for Energy Conversion and Storage and the Korea Institute of Energy and Resources Technology Evaluation and Planning.

References

1. Conway, B. E. *Electrochemical Supercapacitor-Scientific Fundamentals and Technological Application*; Kluwer Academic: New York, 1999; p 29-31.
2. Koetz, R.; Carlen M. *Electrochimica Acta* **2000**, *45*, 2483.
3. Frackowiak, E.; Béguin, F. *Carbon* **2001**, *39*, 937.
4. Fuertes, A. B.; Lota, G.; Centeno, T. A.; Frackowiak, E. *Electrochimica Acta* **2005**, *50*, 2799.
5. Liang, H.; Chen, F.; Li, R.; Wang, L.; Deng, Z. *Electrochimica Acta* **2004**, *49*, 3463.
6. Morita, M.; Goto, M.; Matsuda, Y. *J. Appl. Electrochem.* **1992**, *22*, 901.
7. Tanahashi, T.; Yoshida, A.; Nishino, A. *J. Electrochem. Soc.* **1990**, *137*, 3052.
8. Rudge, A.; Raistrick, I.; Gottesfeld, S.; Ferraris, J. P. *Electrochimica Acta* **1994**, *39*, 273.
9. Rudge, A.; Davey, J.; Raistrick, I.; Gottesfeld, S.; Ferraris, J. P. *J. Power Sources* **1994**, *47*, 89.
10. Hu, C. C.; Su, J. H.; Wen, T. C. *J. of Physics and Chemistry of Solids* **2007**, *68*, 2353.
11. Zhou, Y. K.; He, B. L.; Zhou, W. J.; Huang, J.; Li, X. H.; Wu, B.; Li, H. L. *Electrochimica Acta* **2004**, *49*, 257.
12. Ye, J. S.; Liu, X.; Cui, H. F.; Zhang, W. D.; Sheu, F. S.; Lim, T. M. *Electrochemistry Communications* **2005**, *7*, 249.
13. Show, Y.; Imaizumi, K. *Diamond & Related Materials* **2007**, *16*, 1154.
14. Kim, J. H.; Nam, K. W.; Ma, S. B.; Kim, K. B. *Carbon* **2006**, *44*, 1963.
15. Frackowiak, E.; Metenier, K.; Bertagna, V.; Béguin, F. *Appl. Phys. Lett*. **2000**, *77*, 2421.
16. Frackowiak, E.; Jurewicz, K.; Delpeux, S.; Béguin, F. *J. Power Sources* **2001**, *97*/*98*, 822.
17. Rong, C.; Xien, H. *J. of Colloid and Interface Science* **2005**, *290*, 190.
18. Tashima, D.; Kurosawatsu, K.; Uota, M.; Karashima, T.; Otsubo, M.; Honda, C.; Sung, Y. M. *Thin Solid Films* **2007**, *515*, 4234.
19. Xia, X. H.; Jia, Z. J.; Yu, Y.; Liang, Y.; Wang, Z.; Ma, L. L. *Carbon* **2007**, *45*, 717.
20. Qu, D.; Shi, H. *J. Power Sources* **1998**, *74*, 99.
21. Ryoo, M. W.; Kim, J. H.; Seo, G. *J. of Colloid and Interface Science* **2003**, *264*, 414.
22. Huang, C. W.; Chuang, C. M.; Ting, J. M.; Teng, H. *J. of Power Sources* **2008**, *183*, 406.